Journal of Alloys and Compounds 500 (2010) L22–L25

Contents lists available at ScienceDirect

Journal of Alloys and Compounds

journal homepage: www.elsevier.com/locate/jallcom

Short communication

Influence of Ag micro-alloying on the microstructure and properties of Cu–7Cr in situ composite

Keming Liu[a,b], Deping Lu[b,*], Haitao Zhou[a], Andrej Atrens[c], Zhibao Chen[b], Jin Zou[b], Sumin Zeng[a]

[a] School of Materials Science and Engineering, Central South University, Changsha 410083, PR China
[b] Jiangxi Key Laboratory for Advanced Copper and Tungsten Materials, Jiangxi Academy of Sciences, Nanchang 330029, PR China
[c] The University of Queensland, Materials Engineering, Brisbane, Qld 4072 Australia

ARTICLE INFO

Article history:
Received 8 March 2010
Received in revised form 24 March 2010
Accepted 31 March 2010
Available online 8 April 2010

Keywords:
Cu alloy
In situ composite
Microstructure
Strength
Electrical conductivity

ABSTRACT

This paper studied the influence of Ag micro-alloying on the deformation-processed Cu–7Cr in situ composite, by a comparison of Cu–7Cr and Cu–7Cr–0.07Ag. For both alloys, the as-cast microstructure consisted of a Cu matrix and Cr dendrites; after hot and cold working the microstructure consisted of a Cu matrix containing Cr fibres elongated in the working direction. The as-cast microstructure of the Ag-containing alloy contained finer Cr dendrites. The Ag-containing in situ composite had thinner Cr fibres, higher tensile strength, higher ductility, and slightly higher conductivity. The Cu–7Cr–0.07Ag in situ composite had a good combination of properties: a tensile strength of 772 MPa and a conductivity of 77.3%IACS.

1. Introduction

Heavily drawn binary Cu-based in situ composites such as Cu–Nb, Cu–Ag, Cu–Fe, and Cu–Cr have been the subject of extensive research due to their excellent strength and good conductivity [1–5]. However, Nb and Ag are expensive metals, which impede their use in large-scale applications. Cu–Fe in situ composites have relatively low conductivity because of the relatively high solubility of Fe in Cu at high temperatures, the slow kinetics of iron precipitation at lower temperatures and the particularly harmful effect on the conductivity of iron atoms in solid solution [4]. Cr is a promising reinforcing metal for Cu-based in situ composites due to the relative economical cost, limited solubility in Cu and high tensile strength.

In order to achieve greater strength, higher electrical conductivity and better ductility, a third element such as Zr, Co, or Ag, has been added into the Cu–Cr alloys [6–8]. Deng et al. [6] reported that the addition of 0.4 wt.%Zr to the Cu–10 wt.%Cr in situ composite produced smaller as-cast Cr dendrites, which led to finer filaments at higher strain ratios. Song et al. [7] found that the distance between filaments in Cu–7Cr–0.9Ag was slightly smaller than that of Cu–7Cr–0.9Co. Raabe et al. [8] produced the Cu–10 wt.%Cr–3 wt.%Ag in situ composite with a tensile strength of 1260 MPa combined with a conductivity of 62%IACS.

This paper studied a new class of ternary Cu-base composites, where the noble metals are replaced by Cr, and the Ag content is reduced. The aims of this work were to understand the influence of Ag as a micro-alloying addition, and to determine what combination of properties was possible to produce in a cold worked Ag micro-alloyed Cu–Cr in situ composite.

2. Experimental details

Cu–7Cr and Cu–7Cr–0.07Ag were melted in a vacuum induction furnace and were cast into rod ingots of diameter, d = 36 mm. The starting materials were electrolytic Cu, Cr and Ag, each at least 99.94 wt.% purity. The rod ingots were (i) solution treated at 950 °C for 3 h, (ii) hot rolled at 800 °C in air, (iii) machined to d = 21.5 mm to remove surface oxides and defects, (iv) solution treated at 950 °C for 70 min, (v) cold rolled to d = 9 mm and (vi) wire-drawn. The wire-drawing was as follows: cold drawing (CD) from d = 9 mm to d = 4.5 mm; intermediate heat treatment (IHT) at 550 °C for 30 min; CD to d = 2 mm; IHT at 550 °C for 20 min; CD to d = 0.8 mm; IHT at 650 °C for 10 min; and CD to 0.24 mm. The IHTs. It was found experimentally that grain coarsening (leading to poor final properties) occurred if the annealing temperature was too high and the annealing time too long. However, it was not possible to carry out the next cold deformation if the anneal was at too low a temperature and too short a duration. The cumulative cold deformation strain η was 4, 4.75, 6, 6.58, 8 and 9 for d = 2.92, 2, 1.07, 0.8, 0.39 and 0.24 mm, where $\eta = \ln(A_0/A)$ and A_0 and A are the original and final cross-section areas, respectively.

Microstructures were investigated using an optical microscope and a scanning electron microscope (SEM). The mechanical properties were measured using an electronic tensile-testing machine (EMT2203-B) equipped with an extensometer and using custom designed wire grips. All tensile tests were performed at room

* Corresponding author. Tel.: +86 791 8176237; fax: +86 791 8176237.
E-mail address: llludp@163.com (D. Lu).

0925-8388/$ – see front matter © 2010 Elsevier B.V. All rights reserved.
doi:10.1016/j.jallcom.2010.03.246

temperature using a strain rate of $1.5 \times 10^{-4}\ s^{-1}$. Fracture surfaces of the tensile specimens were examined in a SEM (JSM-6360LV). Electrical resistivity, ρ, was measured at room temperature using a ZY9987 digital micro-ohmmeter with precision of 1 $\mu\Omega$. The corresponding conductivity, σ [%IACS], was evaluated from $\sigma = 172.41/\rho$.

3. Results and discussion

3.1. Microstructure

Fig. 1(a) and (b) presents the microstructure of as-cast Cu–7Cr and Cu–7Cr–0.07Ag alloys, respectively. These two alloys had similar as-cast microstructures. The second-phase Cr dendrites were evenly distributed in the Cu matrix and randomly oriented with respect to the ingot axis. The dendrites of Cu–7Cr–0.07Ag were finer than those of Cu–7Cr, in agreement with Song et al. [9]. Ag is known to wet solid Cr if the oxygen partial pressure is low, which may lower the interface energy and result in easier nucleation of Cr dendrites. The effect of Ag on Cr nucleation in Cu is not clear at present and needs more in-depth investigation.

Fig. 1(c) and (d) respectively presents typical microstructures of longitudinal sections of the deformation-processed Cu–7Cr and Cu–7Cr–0.07Ag in situ composites with $\eta = 4$: Cu matrix plus elongated Cr grains and thin Cr fibres parallel to the drawing direction. The deformation of the Cr dendrites of Cu–7Cr was not uniform; there were still many round Cr grains. In contrast, the Cr dendrites of as-cast Cu–7Cr–0.07Ag had been all drawn into long thin fibres. The more uniform and finer fibres in the Cu–7Cr–0.07Ag in situ composite was attributed to the initial finer dendrite size in the as-cast Cu–7Cr–0.07Ag and the easier refinement of fibres due to a stronger Cu matrix, strengthened by Ag in solid solution. The microstructures of the cold worked in situ composites were similar to those reported in previous studies [10,11]. The initially randomly distributed Cr dendrites in the as-cast microstructure were transformed into Cr fibres aligned parallel to the drawing axis, with fibre aspect ratio increasing with increasing η.

Fig. 1(e) and (f) presents the microstructure of transverse sections of the Cu–7Cr and Cu–7Cr–0.07Ag in situ composite with $\eta = 4$. The fibres of Cu–7Cr–0.07Ag were finer than those of Cu–7Cr in agreement with the microstructures of longitudinal sections. The fibres had a ribbon-like morphology rather than a circular section. This is attributed to the deformation producing Cr fibres with a ⟨1 1 1⟩ fibre texture, which promoted plane strain deformation rather than axially symmetric flow. However, the Cu matrix did deform in an axially symmetric manner during wire-drawing,

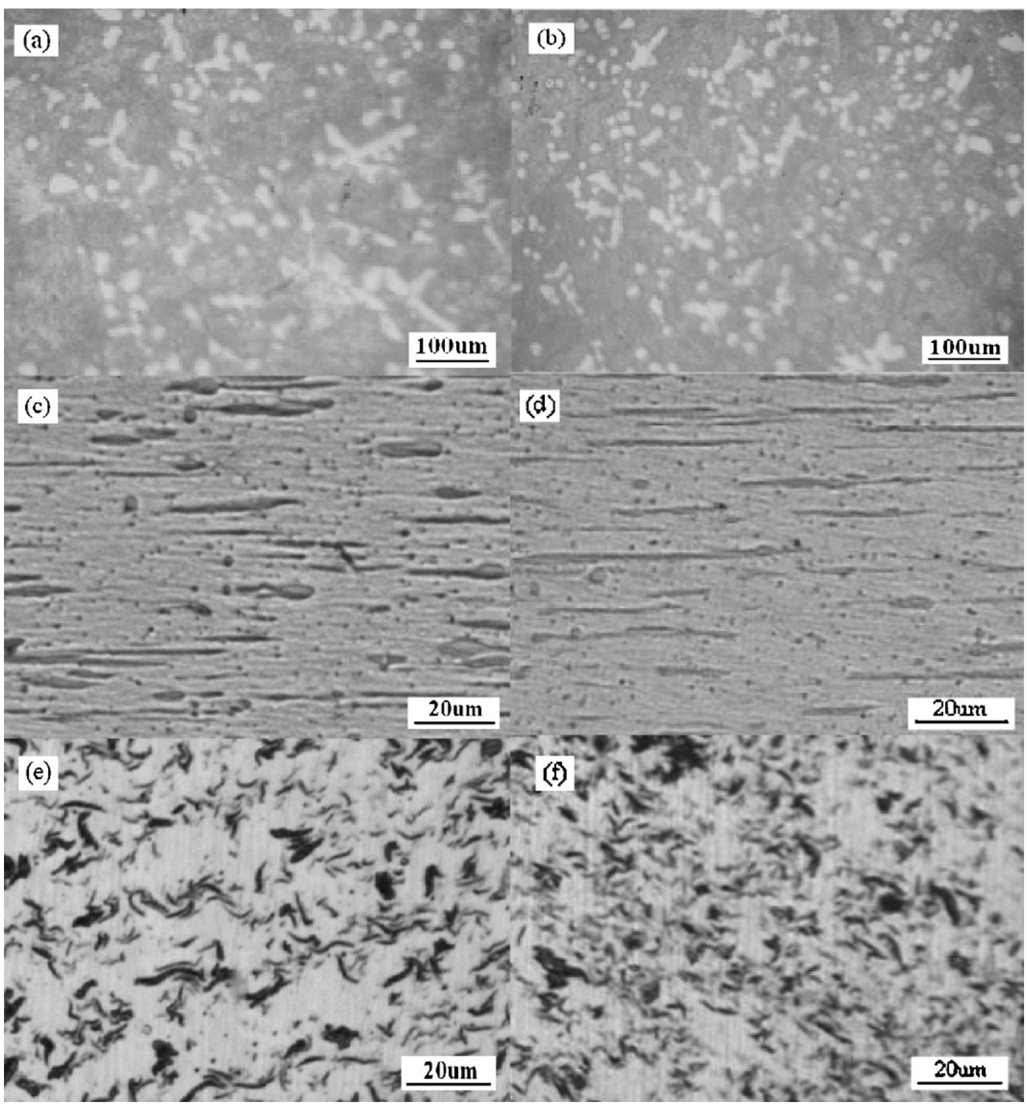

Fig. 1. Microstructures: (a) as-cast Cu–7Cr, (b) as-cast Cu–7Cr–0.07Ag, (c) longitudinal section of the Cu–7Cr in situ composite with $\eta = 4$, (d) longitudinal section of the Cu–7Cr–0.07Ag in situ composite with $\eta = 4$, (e) transverse section of the Cu–7Cr in situ composite with $\eta = 4$, and (f) transverse section of the Cu–7Cr–0.07Ag in situ composite with $\eta = 4$.

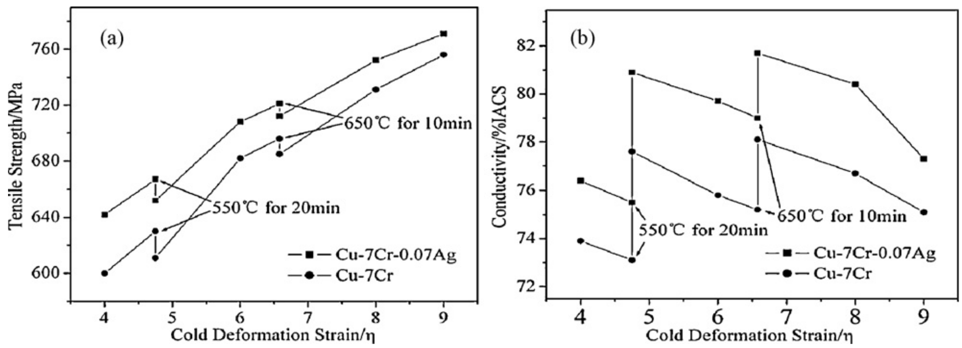

Fig. 2. Tensile strength (a) and conductivity (b) of Cu–7Cr and Cu–7Cr–0.07Ag in situ composites with two IHTs vs deformation strain.

which constrained and forced the Cr fibres to fold or twist about the wire axis to maintain compatibility with the matrix and produced the irregular cross-section.

3.2. Strength and conductivity

Fig. 2(a) and (b) presents the tensile strength and conductivity versus cumulative deformation strain for the Cu–7Cr and Cu–7Cr–0.07Ag in situ composites with two IHTs. This is not to imply that there is a causal relationship between these two parameters as it is expected that the strength and conductivity are determined by the microstructure and chemical composition of the constituent phases. Fig. 2(a) shows that the tensile strength increased with increasing strain. Though the two IHTs decreased the tensile strength, cold drawing, with a large deformation strain, transformed the as-cast microstructure into an in situ composite. The increase in strength with increasing deformation strain is attributed to the decrease of space between fibres, i.e. the strength obeys the Hall–Petch relation and is determined by the fibre spacing [4]. The tensile strength of Cu–7Cr–0.07Ag was 50–20 MPa higher than that of Cu–7Cr. The difference of strength decreased with increasing deformation strain. The higher strength of Cu–7Cr–0.07Ag is attributed to the Ag, which made the Cr dendrite finer, and resulted in fibre formation in Cu–7Cr–0.07Ag at a lower deformation strain.

Fig. 2(b) shows that the conductivity of Cu–7Cr–0.07Ag was about 2–4%IACS higher than that of Cu–7Cr at each deformation strain. The resistivity of the Cu–Cr in situ composites can be evaluated using a parallel-circuit model [12]:

$$\frac{1}{\rho} = \frac{f_{\mathrm{Cu}}}{\rho_{\mathrm{Cu}}} + \frac{f_{\mathrm{Cr}}}{\rho_{\mathrm{Cr}}} \tag{1}$$

where ρ_{Cu} and ρ_{Cu} are the resistivity of the Cu and Cr phase, respectively; and f_{Cu} and f_{Cr} are volume fraction of the Cu and Cr phase, respectively. The contribution to the total resistivity from the Cr fibres was similar for both alloys; Cu–7Cr and Cu–7Cr–0.07Ag had similar amounts of total Cr fibre fraction; i.e. f_{Cr} was the same for both alloys; and the resistivity of Cr is much higher than that of Cu. Therefore, the main difference of the two alloys is attributed to the resistivity of copper matrix, which can be partitioned into the contribution of four main scattering mechanisms [12]:

$$\rho_{\mathrm{M}} = \rho_{\mathrm{PHO}} + \rho_{\mathrm{DIS}} + \rho_{\mathrm{INT}} + \rho_{\mathrm{IMP}} \tag{2}$$

where ρ_{PHO} is the resistivity contribution from phonon scattering, ρ_{DIS} the dislocation scattering, ρ_{INT} interface scattering, and ρ_{IMP} impurity scattering. Composites with the same draw ratio have similar values of ρ_{PHO} and ρ_{DIS}. The interface between the Cu matrix and Cr fibres was similar for the same deformation strain, so the difference in ρ_{INT} between composites was also small. The main differences in the measured resistivity came from the Cr and Ag atoms dissolved in Cu. The increase in the resistivity of Cu caused by dissolved 1 wt.%Cr is bigger than that caused by dissolved 1 wt.%Ag. Therefore, the conductivity of Cu–7Cr–0.07Ag was higher than that of Cu–7Cr. The conductivity of Cu–7Cr and Cu–7Cr–0.07Ag in situ composites increased with increasing deformation strain from $\eta = 4$ to $\eta = 8$, which may be attributed to IHTs after cold drawing to $d = 2$ mm and $d = 0.8$ mm. Each IHT promotes Cr precipitation from the Cu matrix, which decreases the resistivity. In addition recovery and recrystallization during IHTs also reduce the resistivity. In contrast, the conductivity decreased as the deformation strain increased from $\eta = 8$ to $\eta = 9$; this conductivity decrease is attributed to increased dislocation, and increased interface scattering.

3.3. Ductility

The facture surfaces of the tensile samples of the cold worked Cu–7Cr and Cu–7Cr–0.07Ag in situ composites were examined in SEM. In each case, the surfaces represented ductile fracture. The dimples size was smaller for the Cu–7Cr–0.07Ag in situ composite consistent with the smaller fibre size and smaller inter-fibre

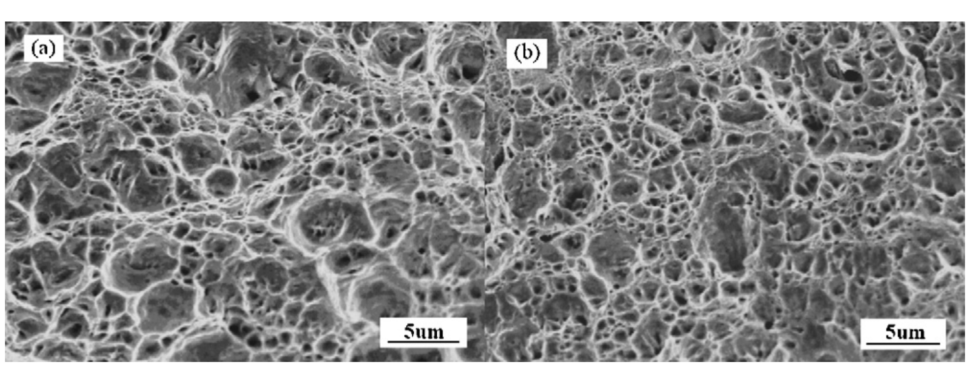

Fig. 3. Fracture surfaces of the Cu–7Cr and Cu–7Cr–0.07Ag in situ composites.

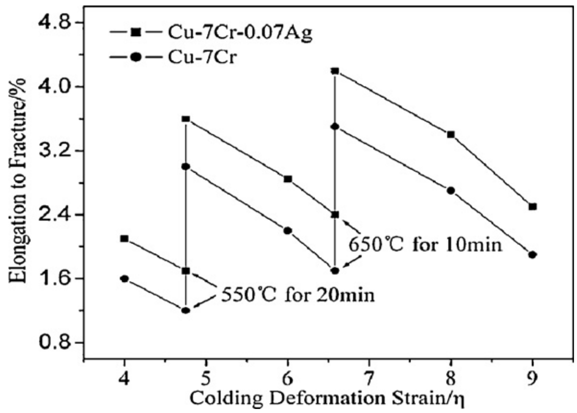

Fig. 4. Elongation to fracture of cold worked Cu–7Cr and Cu–7Cr–0.07Ag in situ composites with two IHTs vs deformation strain.

space. Fig. 3(a) and (b) presents typical fracture surfaces of tensile samples for the particular case of the cold worked Cu–7Cr and Cu–7Cr–0.07Ag with $\eta = 4$. Fig. 4 shows that the elongation to fracture of the Cu–7Cr–0.07Ag in situ composite with two IHTs was higher than that of Cu–7Cr at each deformation strain. The higher ductility of Cu–7Cr–0.07Ag is attributed to its finer microstructure. The elongation to fracture of Cu–7Cr and Cu–7Cr–0.07Ag increased with increasing deformation strain from $\eta = 4$ to $\eta = 8$. This increase is also attributed to the finer microstructure. In contrast, the elongation to fracture decreased as the deformation strain increased from $\eta = 8$ to $\eta = 9$, which may be attributed to work hardening of the copper matrix.

4. Conclusions

Finer Cr dendrites in as-cast microstructure and thinner Cr fibres in deformed microstructure of Cu–7Cr were produced by Ag micro-alloying. The Cu–7Cr–0.07Ag in situ composite had a tensile strength of 772 MPa and a conductivity of 77.3%IACS. The Cu–7Cr–0.07Ag in situ composite had higher ductility and slightly higher conductivity than with the Cu–Cr in situ composite. The increased strength and ductility is attributed to the finer microstructure when the alloy contains Ag. The higher conductivity is attributed to a lower Cr concentration remaining in the Cu matrix when the alloy contains Ag.

Acknowledgements

This project is financially supported by the International Science and Technology Cooperation Project of the Science and Technology Ministry of China (No. 2006DFB53050) and the National Natural Science Foundation of China (No. 50961006), Jiangxi Provincial Department of Science and Technology of China(No. 060009).

References

[1] H.R.Z. Sandim, M.J.R. Sandim, H.H. Bernardi, J.F.C. Lins, D. Raabe, Scripta Mater. 51 (2008) 1099–1104.
[2] A. Gaganov, J. Freudenberger, E. Botcharova, L. Schultz, Mater. Sci. Eng. A 437 (2006) 313–322.
[3] H. Fernee, J. Nairn, A. Atrens, J. Mater. Sci. 36 (2001) 2711–2719.
[4] H.Y. Gao, J. Wang, D. Shu, B.D. Sun, J. Alloys Compd. 438 (2007) 268–273.
[5] A. Vinogradov, V. Patlan, Y. Suzuki, K. Kitagawa, V.I. Kopylov, Acta Mater. 50 (2002) 1639–1651.
[6] J.Q. Deng, X.Q. Zhang, S.Z. Shang, F. Liu, Z.X. Zhao, Y.F. Ye, Mater. Des. 30 (2009) 4444–4449.
[7] J.S. Song, H.S. Kim, C.T. Lee, S.I. Hong, J. Mater. Process. Technol. 130–131 (2002) 272–277.
[8] D. Raabe, K. Miyake, H. Takahar, Mater. Sci. Eng. A. 291 (2000) 186–197.
[9] J.S. Song, S.I. Hong, Y.G. Park, J. Alloys Compd. 388 (2005) 69–74.
[10] L. Zhang, L. Meng, J.B. Liu, Scripta Mater. 52 (2005) 587–592.
[11] D. Raabe, J. Ge, Scripta Mater. 51 (2004) 915–920.
[12] H.Y. Gao, J. Wang, D. Shu, B.D. Sun, Scripta Mater. 54 (2006) 1931–1935.